

Differences in the Behavior of Cytoplasmic Granules and Lipid Bodies during Human Lung Mast Cell Degranulation

ANN M. DVORAK, ILAN HAMMEL, EDWARD S. SCHULMAN, STEPHEN P. PETERS, DONALD W. MACGLASHAN, Jr., ROBERT P. SCHLEIMER, HAROLD H. NEWBALL, KATHRYN PYNE, HAROLD F. DVORAK, LAWRENCE M. LICHTENSTEIN, and STEPHEN J. GALLI

The Departments of Pathology, Beth Israel Hospital and Harvard Medical School, and the Charles A. Dana Research Institute, Beth Israel Hospital, Boston, Massachusetts 02215; Department of Medicine, Division of Clinical Immunology, The Johns Hopkins University School of Medicine at the Good Samaritan Hospital, Baltimore, Maryland 21239; and the Department of Pathology, the Sackler School of Medicine, Tel Aviv University, Ramat Aviv, Israel

ABSTRACT We used a morphometric and autoradiographic approach to analyze changes in specific cytoplasmic granules and cytoplasmic lipid bodies associated with human lung mast cell degranulation. Mast cells were dissociated from lung tissue by enzymatic digestion and were then enriched to purities of up to 99% by countercurrent centrifugation elutriation and recovery from columns containing specific antigen bound to Sepharose 6 MB. Degranulation was induced by goat anti-IgE. At various intervals after stimulation, parallel aliquots of cells were recovered for determination of histamine release or were fixed for transmission electron microscopy. We found that lipid bodies, electron-dense structures that lack unit membranes, were present in both control and stimulated mast cells. Autoradiographic analysis showed that lipid bodies represented the major repository of ³H-label derived from [³H]arachidonic acid taken up from the external milieu. By contrast, the specific cytoplasmic granules contained no detectable ³H-label. In addition, lipid bodies occurred in intimate association with degranulation channels during mast cell activation, but the total volume of lipid bodies did not change during the 20 min after stimulation with anti-IgE. This result stands in striking contrast to the behavior of specific cytoplasmic granules, the great majority of which (77% according to aggregate volume) exhibited ultrastructural alterations during the first 20 min of mast cell activation.

These observations establish that mast cell cytoplasmic granules and cytoplasmic lipid bodies are distinct organelles that differ in ultrastructure, biochemistry, and behavior during mast cell activation.

A previous ultrastructural analysis of human lung mast cell degranulation (4) reported that this process differed from that observed in rat peritoneal mast cells (3, 5, 14, 16, 17, 20). These workers reported that the cytoplasmic granules of human mast cells stimulated with anti-IgE underwent a series of ultrastructural changes that included the transformation from complex granule substructural patterns to a reticular pattern and, finally, the alteration of the granule contents to an amorphous state before discharge. They concluded that the crystalline patterns exhibited by human lung mast cell granules represented storage forms of materials that are solubilized

before fusion of the granule membrane with the plasma membrane and discharge.

While these constitute provocative ideas, our analysis of the published photomicrographs suggested that they were based largely upon the interpretation of cytoplasmic lipid bodies as "solubilized mast cell granules." Lipid bodies are nonmembrane-bound, roughly spherical structures that may occur in a variety of cell types, but which differ from specific secretory granules in genesis and biochemical content, as well as in ultrastructure (11). Although lipid bodies have been reported to occur in human mast cells (1, 6, 23), to our

knowledge a possible role for these structures during degranulation has not previously been studied.

To analyze changes in cytoplasmic lipid bodies associated with human mast cell histamine release, we studied purified populations of mast cells isolated from human lung and then stimulated to degranulate by exposure to anti-IgE *in vitro*. Changes in the volumes of cell organelles were then quantitated in transmission electron micrographs by point counting. These studies confirmed that mast cell histamine release was associated with substantial reduction in the aggregate volume of intact secretory granules. However, degranulation was associated with little or no change in the total volume of cytoplasmic lipid bodies. Furthermore, although occasional lipid bodies appeared to discharge their contents into degranulation channels that were in communication with the extracellular space, we found no evidence of transformation of specific cytoplasmic granules into lipid bodies.

MATERIALS AND METHODS

Isolation of Mast Cells

Mast cells were purified from human lung as previously described (21). Briefly, grossly normal lung fragments were obtained from pneumonectomy or lobectomy specimens removed for pulmonary neoplasm. Single cells were dispersed from lung fragments by two 30-min incubations in solutions containing pronase (2 mg/ml) and chymopapain (0.5 mg/ml) followed by two incubations in solutions containing collagenase (1 mg/ml) and elastase (10 U/ml). Lung cell suspensions containing $6 \pm 0.7\%$ mast cells were enriched to $29 \pm 3.5\%$ mast cells (range 13.5–45%) by countercurrent centrifugation elutriation. Countercurrent centrifugation elutriation fractions with $\geq 25\%$ mast cells were pooled. Mast cells were then passively sensitized with benzylpenicilloyl-specific IgE (6,000 ng/ml), applied to a benzylpenicilloyl-Sepharose 6 MB column, eluted from the column with the monovalent penicillin haptene, *N*- ϵ -benzylpenicilloyl-*N*- α -formyl-L-lysine, and washed in PAG¹ buffer (25 mM piperazine-*N,N'*-bis-2-ethanesulfonic acid [Sigma Chemical Co., St. Louis, MO], 140 mM NaCl, 6 mM KCl, 0.003% human serum albumin [Miles Laboratories, Inc., Elkhart, IN], and 0.1% glucose). Mast cell purity in these preparations was $84 \pm 3\%$ (range 65–99%).

Mast Cell Degranulation

Mast cells were stimulated to degranulate by exposure to antibody to IgE (goat anti-IgE, 2 μ g/ml in PAG buffer plus 1 mM CaCl₂ at 37°C [21]). In four separate experiments, mast cells were incubated with anti-IgE or buffer alone (controls) and fixed for ultrastructural studies 1, 3, 5, 10, 15, 20, and 30 min thereafter. To measure the extent of mast cell degranulation, the supernatants of parallel aliquots of anti-IgE stimulated or control mast cells were analyzed for histamine content by the automated fluorometric technique of Siraganian (22). Total mast cell-associated histamine was determined by lysing aliquots of control cells with 0.4 N perchloric acid. We then calculated the percent of histamine release in control or IgE-stimulated mast cell populations according to the formula: % histamine release = histamine in supernatant + total cell associated histamine.

Transmission Electron Microscopy

We fixed cell suspensions by diluting them in a 10-fold excess of a mixture of 1% paraformaldehyde, 1.25% glutaraldehyde, 0.025% CaCl₂ in 0.1 M sodium cacodylate buffer, pH 7.4 (9). Cells were fixed for 1 h at room temperature, washed, and then suspended in 0.1 M sodium cacodylate buffer, pH 7.4, at 4°C. The cells then were transferred to microtubes, centrifuged at 1,500 *g* for 1 min, suspended in warm 2% agar, and centrifuged again. Some cells were postfixed as a pellet in agar for 2 h at 4°C in 2% aqueous osmium tetroxide and 1.5% potassium ferrocyanide (OPF) in 0.1 M sodium phosphate buffer,

pH 6.0 (9). Other pellets were postfixed for 2 h at room temperature in 2% collidine-buffered osmium tetroxide and stained en bloc with uranyl acetate (OCUB) for 2 h at room temperature (9). Cell pellets were then dehydrated in a graded series of alcohols and embedded in a propylene oxide-Epon sequence. Sections were cut with diamond knives, placed on copper grids, stained with lead citrate, and viewed in a Philips 400 transmission electron microscope.

We cut three randomly placed thin sections from separate blocks of cells exposed to anti-IgE or buffer (controls) for each time interval in each of the four experiments. In all, 117 thin sections were examined in the electron microscope. All mast cells in each grid (~100 cells) were examined at medium to high magnifications (2,800–30,000).

Quantitative Analysis of Mast Cell Degranulation

Two experiments were analyzed quantitatively, using cells from two different donors that gave similar levels of histamine release (~40%). Thin sections from each time point were examined in the same order, beginning at the top left corner of the grid and proceeding to the lower right systematically, until at least 50 recognizable mast cells (nondegranulated or anti-IgE activated) in control or stimulated populations had been photographed. All photomicrographs were printed at $\times 15,000$, and at least 10 prints from each group were selected at random for quantitative analysis by point counting (25). Most mast cell images (e.g., Fig. 1) included part of the nucleus, and one or more cytoplasmic lipid bodies, and multiple specific cytoplasmic granules. For analysis of cell or organelle volumes by point counting (25), multipurpose screens with 1 point/cm² were drawn onto the photomicrographs using a Hewlett-Packard HP86 computer interfaced with a Hewlett-Packard HP 7470 plotter (Hewlett-Packard Co., Palo Alto, CA). We determined the volumes of the entire cell, nucleus, cytoplasmic granules, cytoplasmic lipid bodies, degranulation channels, cytoplasm, and "other" organelles (mitochondria, rough and smooth endoplasmic reticulum, and Golgi structures and cytoplasmic vesicles). The demarcation between a degranulation channel and the plasma membrane was taken as the narrowest constriction of the channel near its apparent point of fusion with the cell surface. The membranes of swollen cytoplasmic granules and chains of interconnected granules containing altered granule matrix material were counted as part of degranulation channels. Mean cell volume (\bar{V}) was calculated from the measured mean profile area (\bar{A}) using the Weibel and Gomez formula: $\bar{V} = 1.4 (\bar{A})^{3/2}$ (24). Nuclear volume (V_N) was estimated by determining the number of points falling on the nucleus (P_N) and the total number of points falling on the cell profile (P_c), and by taking $V_N = (P_N/P_c) \times \bar{V}$. Cytoplasmic volume (V_{CYTO}) was then calculated ($V_{CYTO} = \bar{V} - V_N$) and was used to estimate organelle volumes ($V_o = [P_o/P_{CYTO}] \times V_{CYTO}$). The changes in cell or organelle volume during exocytosis were examined for statistical significance using Student's *t* test.

Autoradiographic Analysis of Mast Cells Labeled with [³H]Arachidonic Acid

We recently reported that several kinds of inflammatory cells, including macrophages, granulocytes, lymphocytes, and mast cells, incorporate ³H-label derived from [³H]arachidonic acid (³H-AA) predominantly into cytoplasmic lipid bodies (6). Because human lung mast cell degranulation is associated with the generation of oxidative products of AA metabolism (19), we used electron microscopic autoradiography to determine whether mast cell activation resulted in alterations of the distribution of ³H-AA-derived label in mast cells allowed to incorporate this precursor over an 18 h period of labeling *in vitro*.

LABELING WITH ³H-AA: Mast cells ($6\text{--}20 \times 10^6$, $92 \pm 2\%$ mast cells) were washed with PAG buffer and then cultured for 18 h in RPMI 1640 medium with 25 mM HEPES; 1 mM glutamine, 10% fetal calf serum, and 100 μ g/ml Kanamycin in a volume of 1.5–2.5 ml in 16 mm flat-bottomed tissue culture wells in humidified 95% air/5% CO₂. Immediately before addition of cells, 50 or 100 μ Ci ³H-AA (NET-398, New England Nuclear, Boston, MA) was placed in each culture well and solvent evaporated under a stream of nitrogen.

STIMULATION OF MAST CELL DEGRANULATION: After 18 h labeling with ³H-AA, mast cells were washed 3 \times with PAG, placed in 0.1 ml of PAG plus 1 mM CaCl₂ at 37°C, and then were stimulated with ionophore A23187 (1 μ g/ml), goat anti-IgE (2 μ g/ml) or, as a control, normal goat serum. After incubation for 15–30 min, cells were diluted in PAG, centrifuged in a microfuge, and the supernatant removed in order to quantitate release of ³H species and histamine. Radioactivity was quantitated by liquid scintillation spectroscopy in a Triton X-100-toluene scintillation cocktail. Histamine was quantitated by an automated fluorometric method (22). Parallel aliquots of ³H-labeled cells were fixed and processed for EM or analyzed for radioactive lipid content by thin layer chromatography (19).

¹ Abbreviations used in this paper: AA, arachidonic acid; BPO-FLYS, *N*- ϵ -benzylpenicilloyl-*N*- α -formyl-L-lysine; EM, electron microscopy; OCUB, osmium collidine uranyl en bloc; OPF, osmium tetroxide-potassium ferrocyanide; PAG buffer, 25 mM piperazine-*N,N'*-bis-2-ethanesulfonic acid, 140 mM NaCl, 6 mM KCl, 0.003% human serum albumin, and 0.1% glucose.

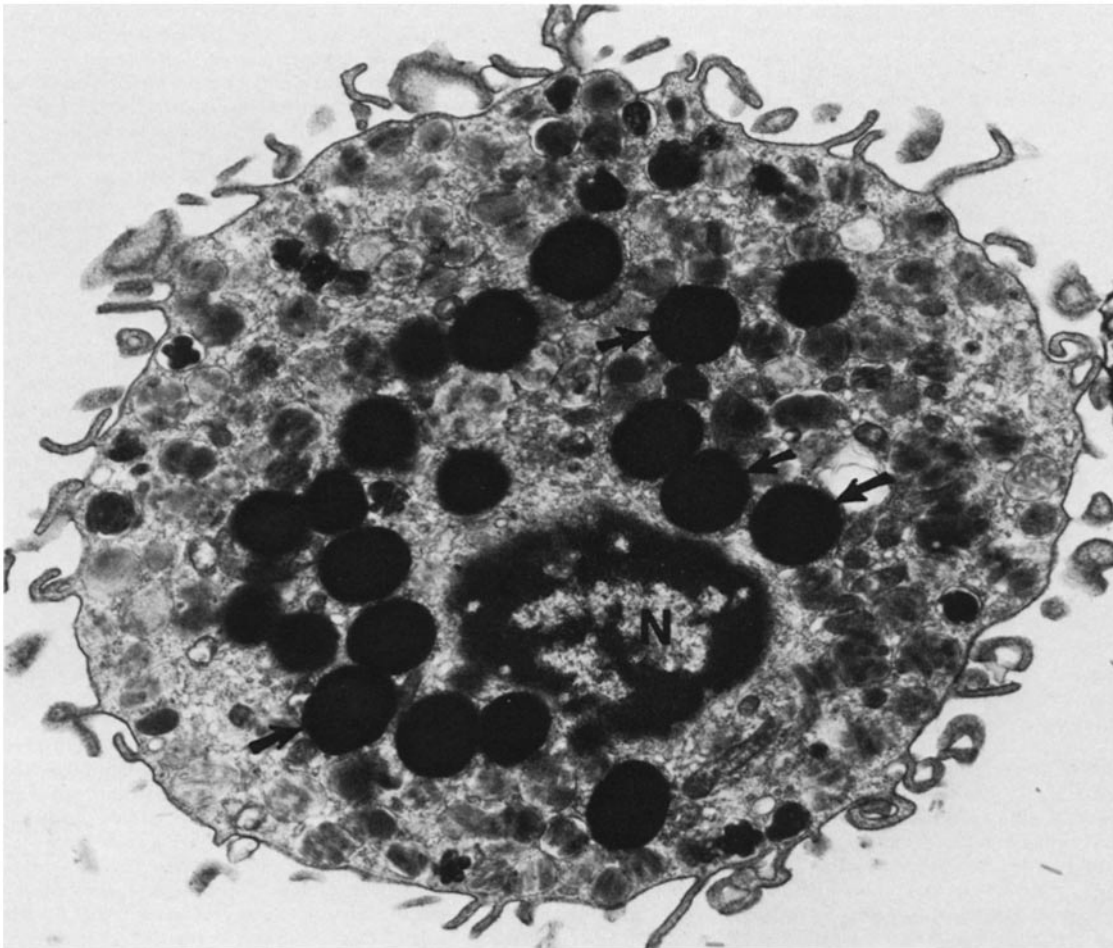


FIGURE 1 Control mast cell illustrating cytoplasmic granules containing scroll-like inclusions and several large cytoplasmic lipid bodies (arrows). O.C.U.B. $\times 6,000$.

ANALYSIS OF ULTRASTRUCTURAL AUTORADIOGRAPHY: Electron microscopic autoradiographs were prepared by looping 100 nm thick sections on copper grids with Ilford L-4 emulsion. (Ilford Ltd., Ilford, Essex, England). These were then exposed at 4°C, developed in Microdol-X and stained in lead (6). Chi-square analysis was performed on electron microscope prints magnified to $\times 16,200$ to determine whether an association existed between cell organelles and silver grains (26). A standard grid composed of circles ($r = 260$ nm, approximately the size of specific mast cell granules and smaller than all other structures analyzed) with a center-to-center distance of 2 cm was employed for morphometric analysis (grain counting).

RESULTS

Control Mast Cells

Unlike rat peritoneal mast cells, whose cytoplasmic granules are homogeneously electron dense and therefore present a uniform ultrastructural appearance (5, 17, 20), human mast cell granules may exhibit a variety of different ultrastructural patterns (1, 2, 4, 13, 15, 18, 23). In our preparations, the most common of these consisted of granules with one to many cylindrical scroll-like inclusions (Fig. 1, Fig. 2, *A* and *B*). The scrolls themselves varied in overall electron density (Fig. 2*A*), and some scrolls contained central deposits of homogeneously electron dense matrix (Fig. 2, *A* and *B*). Because scrolls with central densities appeared in both control and in anti-IgE stimulated mast cells, we do not consider this finding evidence of an early stage of granule dissolution. Some granules had

crystalline (Fig. 2*C*), particulate (Fig. 2*D*) or reticular (Fig. 3, *A-C*) patterns. Although the reticular pattern has been attributed to dissolution of highly ordered granule contents (4), we observed a small number (<5%) of granules with this ultrastructure in both control and stimulated mast cell preparations. A few individual granules of occasional (<5%) control mast cells were swollen and contained separated or distended scrolls and/or scant particulate electron dense material (cf. in Fig. 3, *D* and *E*). These changes were similar to those characteristic of the majority of granules at early intervals after mast cell stimulation with anti-IgE; their presence in a small minority of control mast cells may have reflected prior stimulation or secretory activity, occurring either *in vivo* or during the cell isolation procedure.

In addition to specific cytoplasmic granules, control mast cells also contained cytoplasmic lipid bodies (Fig. 1 and 3*F*). Lipid bodies are roughly spherical, variably dense structures that are often enmeshed in cytoplasmic filaments and that, on average, are larger and less numerous than the specific cytoplasmic granules. They also differ from granules in that they lack a unit membrane (Fig. 3*F*). They have been identified in the mast cells of human adenoids (1) and in human nasal and bronchial mucosal mast cells (23), and are seen regularly as a component of the cytoplasm of human lung mast cells (6). We have never observed them in human skin mast cells (A. M. Dvorak, unpublished data).

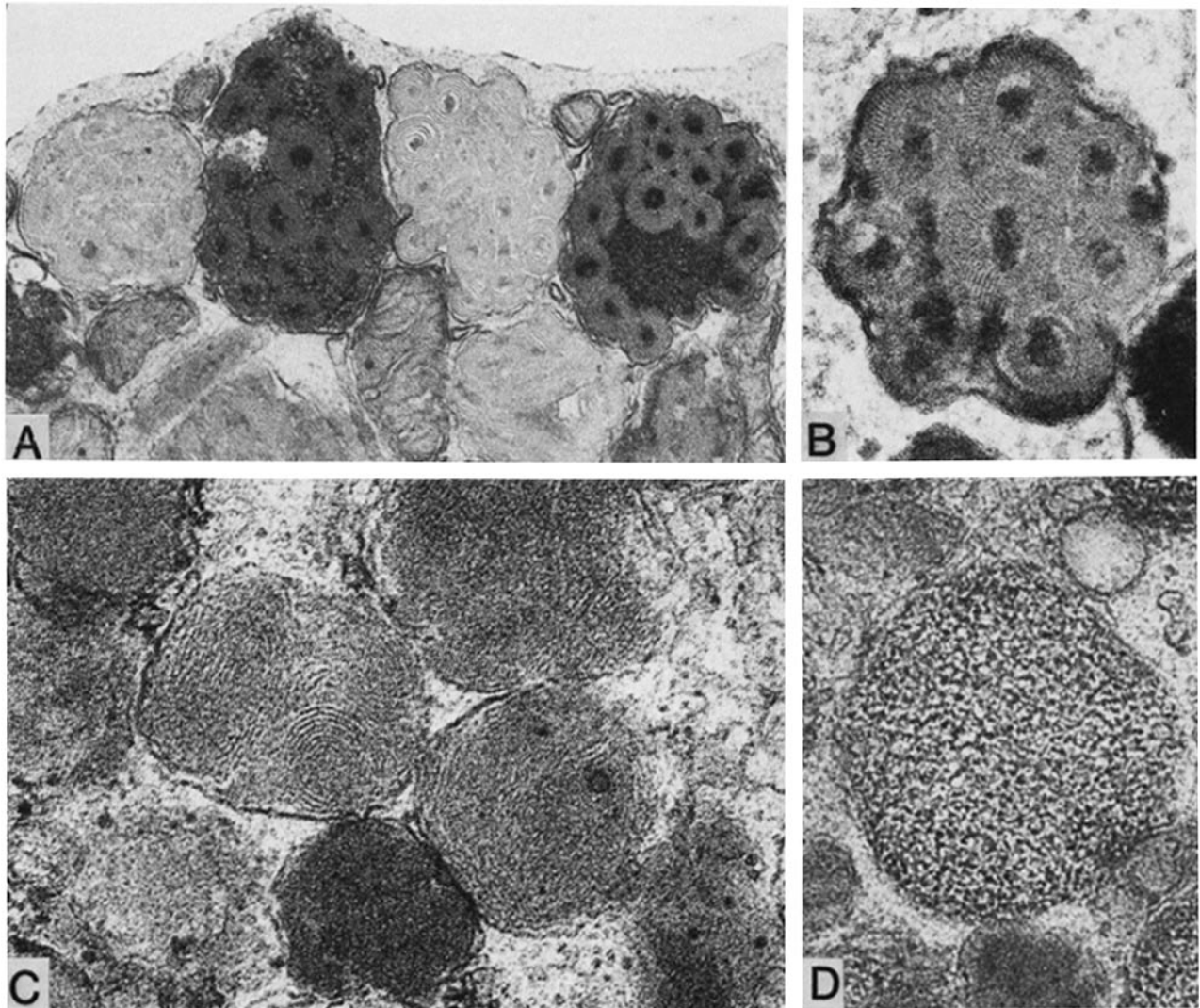


FIGURE 2 High power electron micrographs of scroll (A and B), crystal (C), or particle (D) containing granules from control mast cells. Scroll-containing granules vary in overall electron density (A); many scrolls exhibit central homogeneously electron-dense material (A and B). Many scrolls also have a periodic striation at their periphery (A and B). Crystalline granule content presents regular straight or curved parallel arrays oriented in multiple directions (C). Granules containing particles exhibit variable amounts of electron-lucent space separating electron-dense particles (D). (A-D) OPF. (A) $\times 52,000$; (B) $\times 121,000$; (C) $\times 78,000$; (D) $\times 63,500$.

Mast Cells Stimulated by Anti-IgE

Activation of mast cells by anti-IgE resulted in a characteristic set of ultrastructural alterations whose final effect was to expose the cytoplasmic granule interiors to the external milieu. Although these changes constituted a continuum, and individual mast cells occasionally demonstrated several of them simultaneously, they could be ordered into the following sequence: (a) Cytoplasmic granule swelling and fusion. As early as 1 min (Fig. 4A) and prominently by 3 min after exposure to anti-IgE, cytoplasmic granules appeared swollen and, in favorable planes of section, clearly demonstrated areas of membrane fusion with adjacent granules. Initially, prestimulation matrix configurations such as scrolls, particles, crystals, and occasional reticular patterns were still identifiable in these granules, although their substructural elements progressively separated from one another. (b) Formation of chains of interconnected granules, which enlarged to form tortuous cytoplasmic channels containing altered granule ma-

trix material (Fig. 4B). This change was observed rarely as early as 1 min after administration of anti-IgE, and was marked by 3 min. (c) Fusion of channels with the plasma membrane. Although open channels sometimes contained altered granule matrix material, neither membrane-free granules nor identifiable granule constituents (such as scrolls, crystals, particles, or reticular structures) was ever observed either free in the extracellular medium or attached to the surface of degranulating mast cells. This is in contrast to the degranulation patterns of rat peritoneal mast cells (16, 20), and human (8) or guinea pig basophils (7), where recognizable granule structures are extruded to the exterior.

As noted by many others (1, 4, 15, 16, 23), mast cell degranulation was associated with striking increases in cytoplasmic filaments, particularly in the paranuclear region. In our material, many filaments were intimately associated with cytoplasmic lipid bodies. Despite marked reductions in the number of cytoplasmic granules during anti-IgE induced secretion, the numbers of cytoplasmic lipid bodies changed little

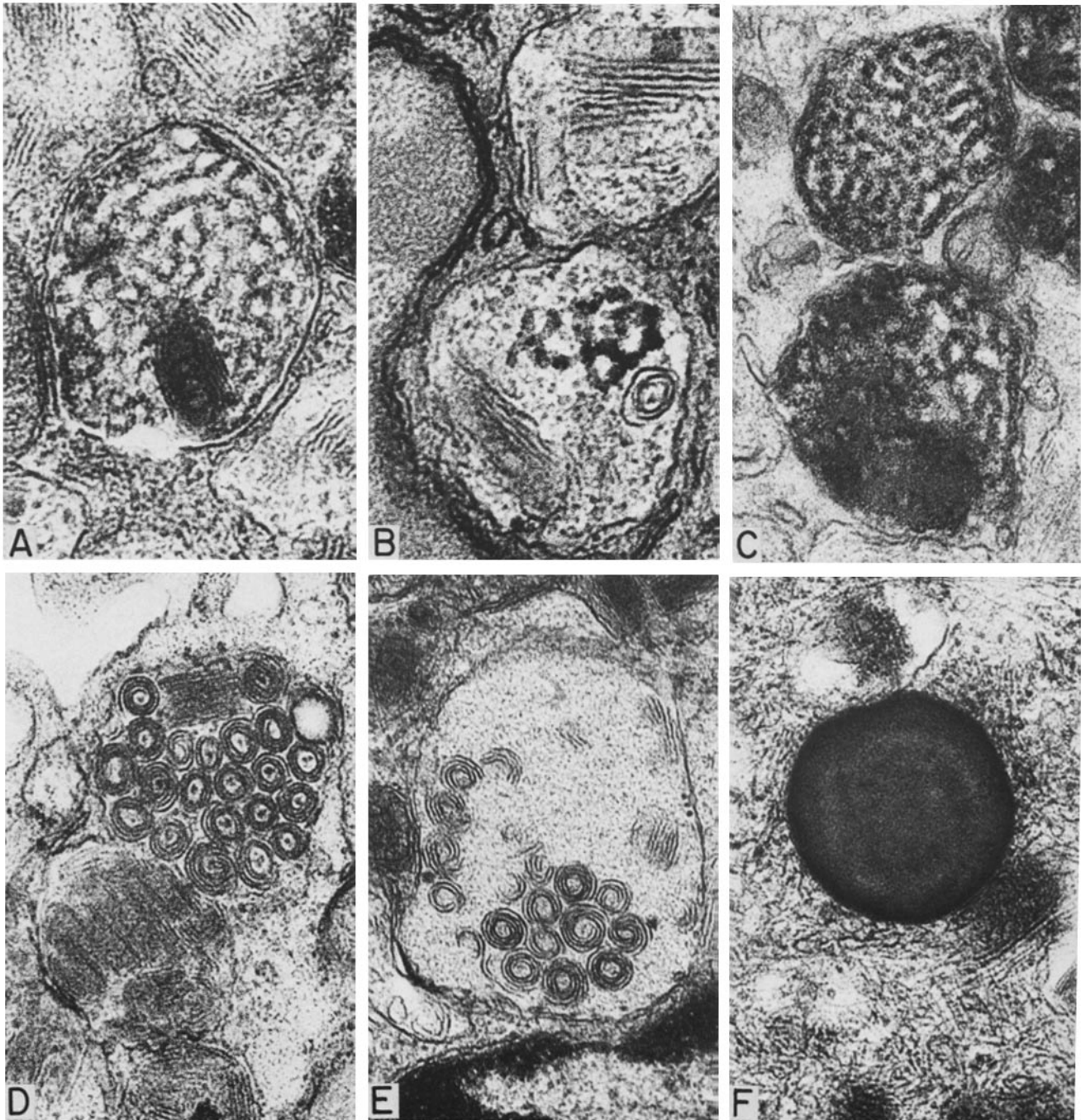


FIGURE 3 (A-E) Granules of control mast cells 0-10 min after incubation in buffer (6-7% histamine release). (A-C) Coarse thread-like or "reticular" patterns. (D) Scrolls with central densities. (E) A swollen granule with a mixture of scrolls, scroll fragments, and small particles. (F) A typical cytoplasmic lipid body; in contrast to the granules, it is homogeneously electron-dense, lacks a unit membrane, and is surrounded by cytoplasmic filaments. (A) OCUB, $\times 75,000$; (B) OPF, $\times 76,500$; (C) OPF, $\times 62,500$; (D) OPF, $\times 63,000$; (E) OCUB, $\times 55,000$; (F) OCUB, $\times 54,000$.

or not at all (see below). At late stages of degranulation, some lipid bodies appeared close to degranulation channels (Fig. 4B) or, rarely, the plasma membrane. In a few instances we observed apparent discharge of osmiophilic content from lipid bodies into degranulation channels (Fig. 5), but we never observed discharge of lipid bodies from the cell surface. We also found no evidence of transformation of membrane-bound cytoplasmic granules into lipid bodies, such as organelles of intermediate ultrastructural appearance.

Quantitative Changes in Mast Cell Organelles during Degranulation

The two separate experiments analyzed gave very similar results that were pooled for presentation in Fig. 6. Mast cells responding to stimulation with anti-IgE exhibited a 77% diminution in the volume of unaltered cytoplasmic granules (Fig. 6). Part of this volume was shifted into that of the degranulation channels, which we classified as "intracellular"

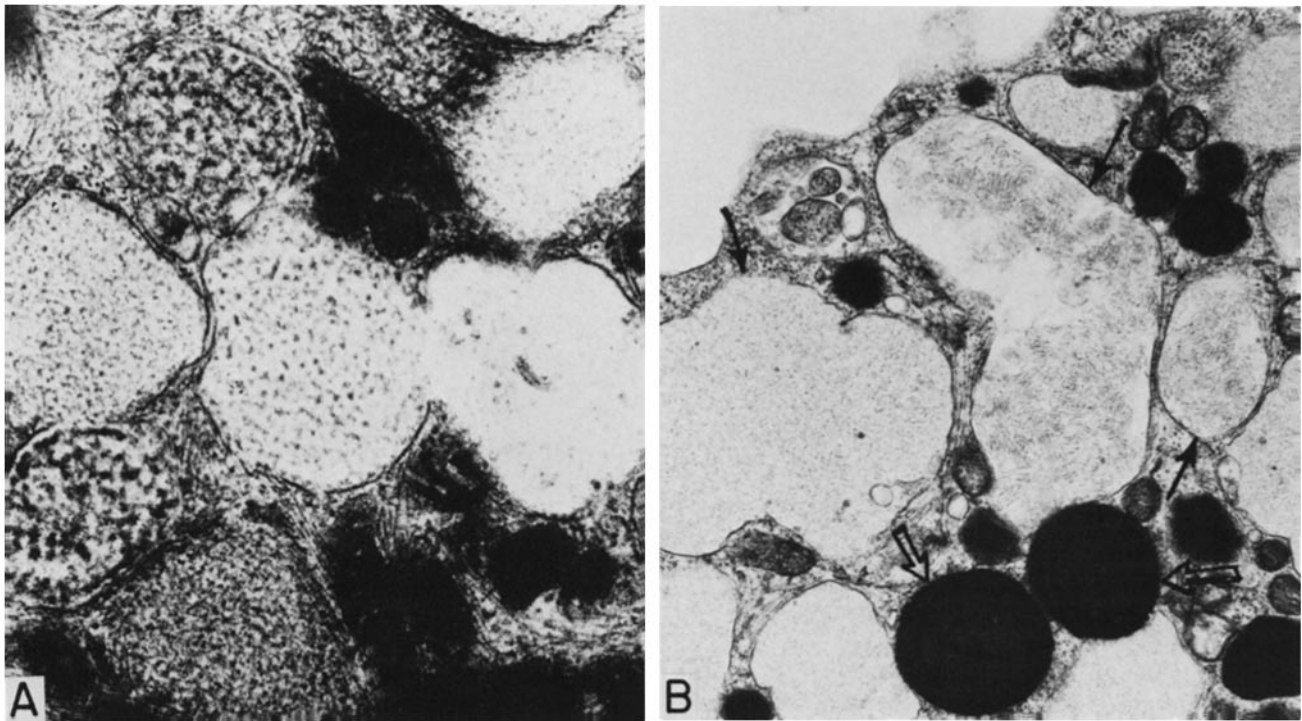


FIGURE 4 High magnification micrographs of mast cells fixed 1 min (A) or 20 min (B) after exposure to anti-IgE. In A, fused granules exhibit loosely packed granule matrix resembling particulate content. In B, intracytoplasmic channels (arrows) contain altered scroll granule matrix. Lipid bodies (open arrows) occupy positions adjacent to degranulation channels. (A) OCUB, $\times 46,500$; (B) OCUB, $\times 21,000$.

(although in strict topological terms, channels that have fused with the plasma membrane may be considered to be outside the cell). The remainder of the loss in granule volume probably accounted for the small (but statistically insignificant) reduction in total cellular volume associated with degranulation (Fig. 6). Degranulation did not result in a significant change in the volume of cytoplasmic lipid bodies (Fig. 6). Quantitative analysis of unstimulated mast cells used as control preparations in these two experiments detected no significant changes in cell or organelle volumes 5 or 20 min after incubation in buffer (data not shown).

Distribution of $^3\text{H-AA}$ Label in Control and Degranulated Mast Cells

Morphometric analysis of EM autoradiographs confirmed the results of our previous experiments (6), showing that nearly all ^3H -label derived from $^3\text{H-AA}$ incorporated by cultured human mast cells during an 18 h incubation in vitro was localized to cytoplasmic lipid bodies (Table I, Fig. 7A). Lipid bodies were the only cellular structure exhibiting statistically significant labeling; little or no label was associated with cell membranes. In this experiment, anti-IgE-stimulated mast cells induced ultrastructural changes similar to those described above, including the close approximation of mast cell lipid bodies with degranulation channels (Fig. 7C). Although lipid body contents and autoradiographic grains (Fig. 7B and C) were sometimes observed within degranulation channels, mast cell degranulation appeared to be associated with relatively little net loss of lipid body content. Thus, stimulation with anti-IgE provoked the discharge of only a

small fraction (mean of five experiments, 3%; range 2–12%) of total cell-associated ^3H -lipids (19). In addition, EM autoradiography and morphometric analysis failed to document either statistically significant autoradiographic labeling of degranulation channels (Table I) or significant changes in the overall volume of lipid bodies in mast cells exhibiting degranulation (Fig. 6). In contrast to the small amount of total ^3H -lipid products released by stimulated mast cells in these experiments, there was substantial release of the granule-associated mediator histamine ($\sim 75\%$ release in three experiments with anti-IgE, with spontaneous release in the absence of anti-IgE of $< 5\%$).

DISCUSSION

We found that mast cells derived from human lung, like those identified in other human tissues (1, 23), contained both specific granules and lipid bodies. As in other cells (11), mast cell lipid bodies appear in electron micrographs as round, osmiophilic, nonmembrane-bound structures. In both control and degranulating mast cells, lipid bodies were distributed predominantly near the nucleus, generally in intimate association with cytoplasmic filaments. In addition to differing from cytoplasmic granules in ultrastructure, mast cell lipid bodies also differ from specific granules in size, number, and apparent growth mechanism.²

During degranulation, cytoplasmic granules exhibited a

² Hammel, I., A. M. Dvorak, S. P. Peters, E. S. Schulman, H. F. Dvorak, L. M. Lichtenstein, and S. J. Galli, submitted for publication.

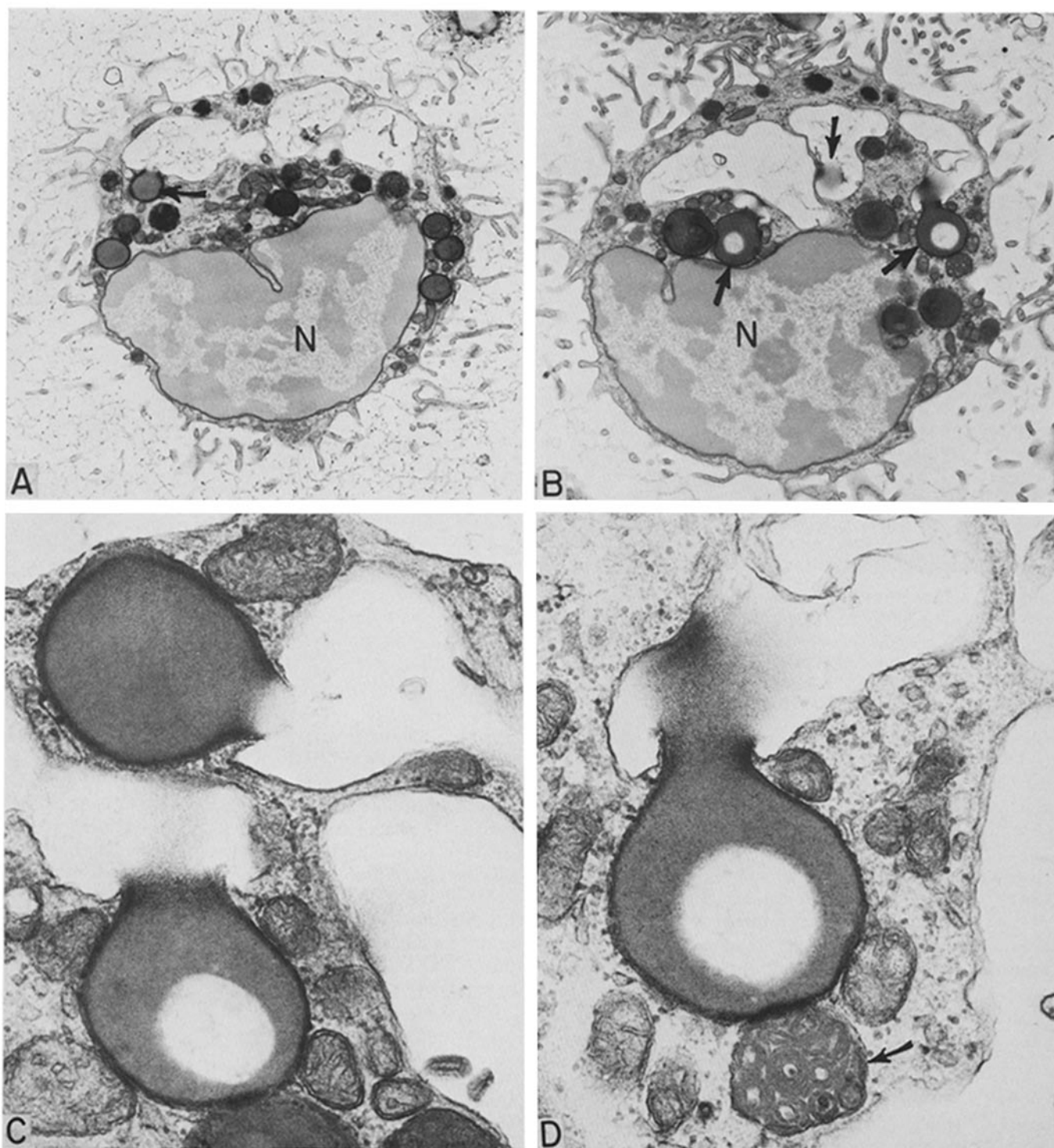


FIGURE 5 Mast cells 20 min after stimulation (42% histamine release) showing discharge of lipid bodies into degranulation channels. In (A and B), multiple lipid bodies (arrows) appear to be discharging into degranulation channels that also contain agar, indicating communication with the extracellular space. (C and D) Higher power electron photomicrographs of lipid bodies discharging into degranulation channels. The arrow in D indicates an unaltered scroll-filled granule. (A-D) OPF. (A and B) $\times 9,500$; (C) $\times 53,000$; (D) $\times 51,000$.

series of characteristic changes including swelling, intergranule fusion to form degranulation channels, and fusion of channels with the plasma membrane. A similar sequence has been proposed by Trotter and Orr (18, 23), who examined

mast cells in biopsies of human nasal and bronchial mucosa. These qualitative changes were accompanied by a precipitous reduction in the number of intact cytoplasmic granules and by substantial histamine release. Throughout the early stages

FIGURE 6 Quantitative analysis of human lung mast cell cellular and organelle volumes before and 5 or 20 min after stimulation with anti-IgE in vitro. Electron micrographs were printed at $\times 15,000$ and point counting was used to calculate the cell volume and the volumes of the nucleus, the specific granules, the degranulation channels, the lipid bodies, the other organelles (mitochondria, rough and smooth endoplasmic reticulum, Golgi structures, and vesicles), and the residual cytoplasm. Cells from two experiments that gave similar levels of mast cell stimulation, as judged by histamine release (see inset), were analyzed. At least 10 prints were analyzed at each time point in each experiment. The two experiments gave similar results which were pooled and are presented as $M \pm SE$. Significant changes in organelle volume associated with degranulation are indicated (Student's *t* test). Morphometric analysis of control mast cells exposed to goat serum instead of anti-IgE disclosed no change in this volume of the cell or any of the organelles over the duration of the experiment (data not shown).

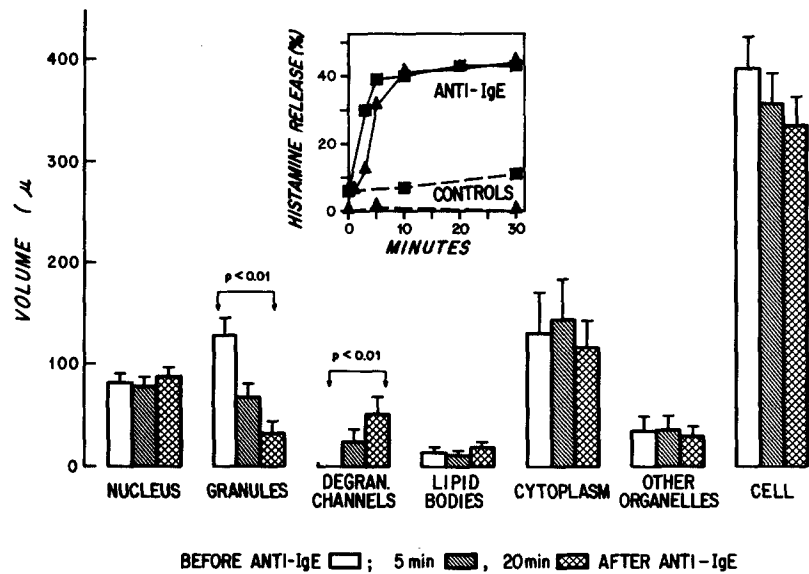


TABLE I
Distribution of Silver Grains in EM Autoradiographs of Human Lung Mast Cells Labeled with $^3\text{H-AA}^*$

Organelle	Control mast cells			Degranulated mast cells		
	percent observed	percent expected	χ^2	percent observed	percent expected	χ^2
Lipid bodies	33.2	4.1	51.2	26.4	2.7	75.0
Granules	23.1	28.3	0.04	10.8	11.6	0.05
Degranulation channels	—	—	—	21.0	23.8	0.14
Cytoplasm	36.1	43.2	0.03	33.4	39.0	0.02
Nucleus	5.8	16.2	0.41	5.7	13.9	0.35
Extracellular	1.9	8.3	0.72	2.7	8.9	0.48

* Mast cells were labeled with $^3\text{H-AA}$ for ~ 18 h in vitro, then fixed for preparation of EM autoradiographs (see Materials and Methods) 15 min after exposure to $2 \mu\text{g/ml}$ anti-IgE (degranulated mast cells) or equivalent normal goat serum (control mast cells). The percent of actual (i.e., observed) organelle-associated silver grains was compared to the percent of grains expected to occur over these structures by chance, assuming a uniform distribution of grains over the prints. The data were derived from 14 control mast cells (with 386 grains) and 12 degranulated mast cells (with 205 grains). Too few grains were associated with cellular membranes to permit formal statistical analysis. The labeling of lipid bodies in control or degranulated mast cells was highly significant ($P < 0.01$) by the χ^2 test. No other structure was significantly labeled (all P values $\gg 0.05$).

of this process, individual granules generally retained a semblance of their characteristic structure (e.g., scroll pattern), but no evidence of their transformation into a homogeneously electron-dense state was observed. Lipid bodies retained their distinctive ultrastructural features during the degranulation process. Although individual lipid bodies bulged against the membrane of degranulation channels and rarely even discharged lipid into these structures, the aggregate volume of lipid bodies did not change significantly. Further, we did not observe any structures that could be interpreted as intermediate between granules and lipid bodies in ultrastructural characteristics. In addition to these strictly morphologic observations, autoradiography showed that lipid bodies repre-

sented the major repository of ^3H -label derived from $^3\text{H-AA}$ and other ^3H -fatty acids (6) incorporated by mature human lung mast cells in vitro. By contrast, the cytoplasmic granules of these mast cells contained no detectable ^3H -label. Together with our other findings, these data strongly support the view (1, 23) that lipid bodies and specific mast cell granules represent distinct organelles, not different functional stages of the same entity.

However, we agree with Caulfield et al. (4) that initiation of mast cell granule matrix solubilization may be among the earliest morphologic events in anti-IgE induced mast cell degranulation, perhaps even preceding fusion of granule membranes with the plasma membrane. In this paper, the earliest ultrastructural evidence of impending degranulation was granule swelling with widening and separation of scroll-like or other granule matrix substructural patterns. It is not clear, however, exactly how this initial solubilization is effected and whether it requires exposure of granule contents to extracellular fluid. In our experience (A. M. Dvorak, unpublished data), the great majority of granules exhibiting swelling and matrix dissolution at early intervals after stimulation do not admit the extracellular tracer, cationized ferritin, when it is incubated with fixed cells. However, exposure of the cytoplasmic granule matrix to the external medium theoretically may be effected by channels too narrow or transient to be identified readily with cationized ferritin. Alternatively, the granule interiors may come into contact with solvent transported from the exterior via traffic of cytoplasmic vesicles (10, 12). In view of these uncertainties, we feel that it is premature to conclude precisely when, in the sequence of human lung mast cell degranulation, the cytoplasmic granule interiors become exposed to the extracellular medium.

These studies were supported in part by U. S. Public Health Service grants CA 28834, AI 07290, HL 23586, and an Arthritis Foundation Postdoctoral Fellowship to Ilan Hammel.

This is publication No. 572 from the O'Neill Laboratories at the Good Samaritan Hospital.

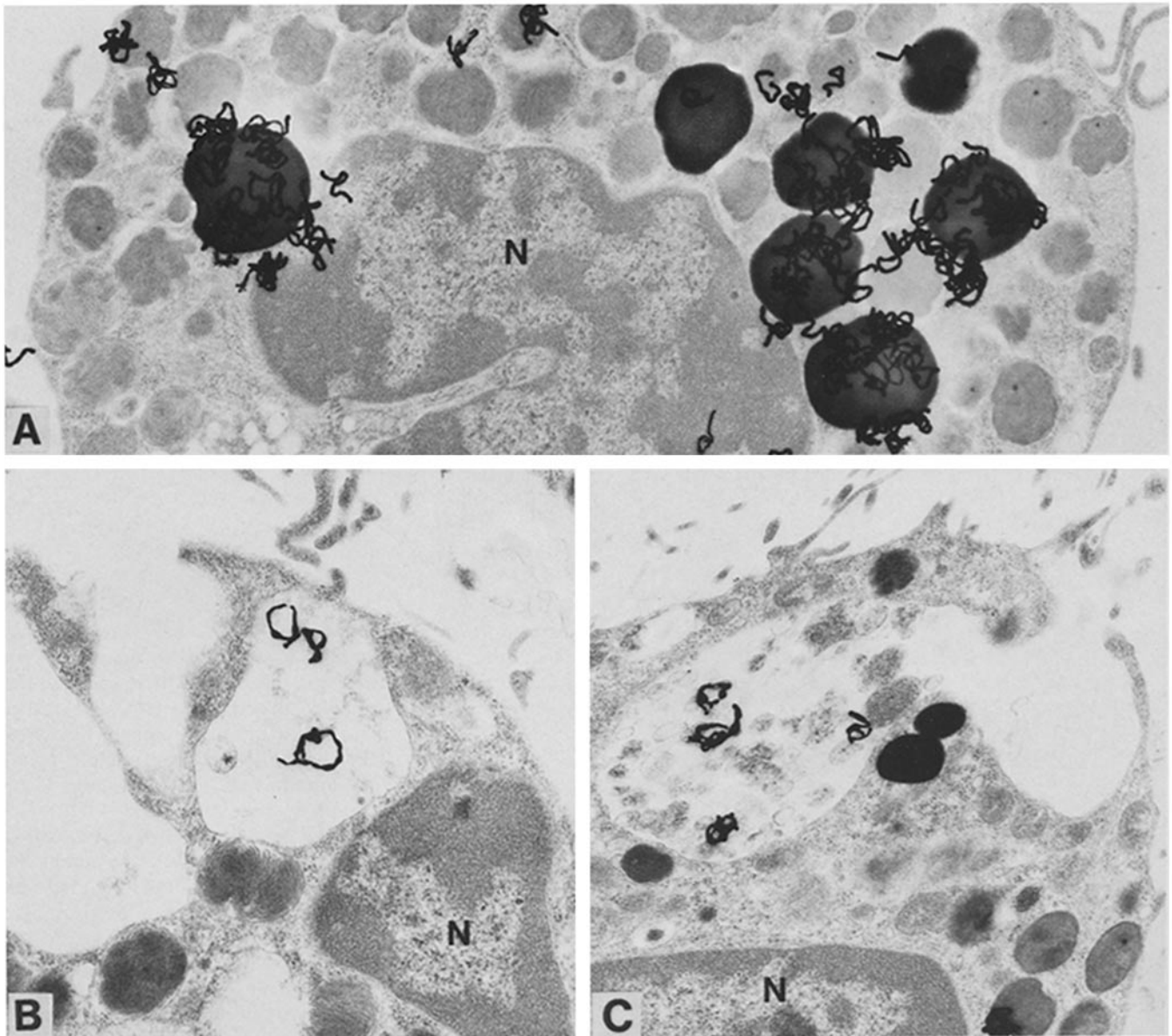


FIGURE 7 (A-C) Electron microscopic autoradiographs of purified human lung mast cells labeled with $^3\text{H-AA}$ in vitro and then exposed to buffer (A) or to anti-IgE (B and C) for 15 min before fixation. The control cell (A) contains heavily labeled lipid bodies, which appear larger and much darker than the more numerous specific cytoplasmic granules. The cells stimulated with anti-IgE (B and C) exhibit labeled degranulation channels that contain altered granule material. N, nucleus. (A-C) OCUB. (A) $\times 17,000$; (B) $\times 21,500$; (C) $\times 17,000$.

Received for publication 20 December 1983, and in revised form 16 July 1984.

REFERENCES

- Behrendt, H., U. Rosenkranz, and W. Schmutzler. 1978. Ultrastructure of isolated human mast cells during histamine release induced by ionophore A 23187. *Int. Arch. Allergy Appl. Immunol.* 56:188-192.
- Brinkman, G. L. 1968. The mast cell in normal human bronchus and lung. *J. Ultrastruct. Res.* 23:115-123.
- Burwen, S. J., and B. H. Satir. 1977. Plasma membrane folds on the mast cell surface and their relationship to secretory activity. *J. Cell Biol.* 74:690-697.
- Caulfield, J. P., R. A. Lewis, A. Hein, and K. F. Austen. 1980. Secretion in dissociated human pulmonary mast cells. *J. Cell Biol.* 85:299-312.
- Chandler, D. E., and J. E. Heuser. 1980. Arrest of membrane fusion events in mast cells by quick-freezing. *J. Cell Biol.* 86:666-674.
- Dvorak, A. M., H. F. Dvorak, S. P. Peters, E. S. Schulman, D. W. MacGlashan, Jr., K. Pyne, V. S. Harvey, S. J. Galli, and L. M. Lichtenstein. 1983. Lipid bodies: cytoplasmic organelles important to arachidonate metabolism in macrophages and mast cells. *J. Immunol.* 131:2965-2976.
- Dvorak, A. M., S. J. Galli, E. Morgan, A. S. Galli, M. E. Hammond, and H. F. Dvorak. 1981. Anaphylactic degranulation of guinea pig basophilic leukocytes. I. Fusion of granule membranes and cytoplasmic vesicles. Formation and resolution of degranulation sacs. *Lab. Invest.* 44:174-191.
- Dvorak, A. M., H. H. Newball, H. F. Dvorak, and L. M. Lichtenstein. 1980. Antigen-induced IgE-mediated degranulation of human basophils. *Lab. Invest.* 43:126-139.
- Dvorak, A. M., M. E. Hammond, H. F. Dvorak, and M. J. Karnovsky. 1972. Loss of cell surface material from peritoneal exudate cells associated with lymphocyte-mediated inhibition of macrophage migration from capillary tubes. *Lab. Invest.* 27:561-574.
- Dvorak, A. M., M. E. Hammond, E. Morgan, N. S. Orenstein, S. J. Galli, and H. F. Dvorak. 1980. Evidence for a vesicular transport mechanism in guinea pig basophilic leukocytes. *Lab. Invest.* 42:263-276.
- Fawcett, D. W. 1981. *The Cell*. W. B. Saunders Co., Philadelphia. 2nd edition. 655-667.
- Galli, S. J., A. M. Dvorak, and H. F. Dvorak. 1984. Basophils and mast cells: morphologic insights into their biology, secretory patterns, and function. *Prog. Allergy* 34:1-141.
- Kawanami, O., V. J. Ferrans, J. D. Fulmer, and R. G. Crystal. 1979. Ultrastructure of pulmonary mast cells in patients with fibrotic lung disorders. *Lab. Invest.* 40:717-735.
- Kinsolving, C. R., A. R. Johnson, and N. C. Moran. 1975. The uptake of a substituted acridine by rat mast cells in relationship to histamine release: a possible indicator of exocytosis-induced expansion of the plasma membrane. *J. Pharmacol. Exp. Ther.* 192:654-669.

15. Kobayasi, T., K. Midtgård, and G. Asboe-Hansen. 1968. Ultrastructure of human mast cell granules. *J. Ultrastruct. Res.* 23:153-165.
16. Lagunoff, D. 1972. Contributions of electron microscopy to the study of mast cells. *J. Invest. Dermatol.* 58:296-311.
17. Lagunoff, D. 1973. Membrane fusion during mast cell secretion. *J. Cell Biol.* 57:252-259.
18. Orr, T. S. C. 1977. Fine structure of the mast cell with special reference to human cells. *Scand. J. Respir. Dis.* 98(Suppl.) 1-7.
19. Peters, S. P., D. W. MacGlashan, Jr., E. S. Schulman, R. P. Schleimer, E. C. Hayes, J. Rokach, N. F. Adkinson, Jr., and L. M. Lichtenstein. 1984. Arachidonic acid metabolism in purified lung mast cells. *J. Immunol.* 132:1972-1979.
20. Röhlich, P., P. Anderson, and B. Uvnäs. 1971. Electron microscopic observations on compound 48/80-induced degranulation in rat mast cells: evidence for sequential exocytosis of storage granules. *J. Cell Biol.* 51:465-483.
21. Schulman, E. S., D. W. MacGlashan, Jr., S. P. Peters, R. P. Schleimer, H. H. Newball, and L. M. Lichtenstein. 1982. Human lung mast cells: purification and characterization. *J. Immunol.* 129:2662-2667.
22. Siraganian, R. P. 1974. An automated continuous flow system for the extraction and fluorometric analysis of histamine. *Anal. Biochem.* 57:383-394.
23. Trotter, C. M., and T. S. C. Orr. 1973. A fine structure study of some cellular components in allergic reactions. I. Degranulation of human mast cells in allergic asthma and perennial rhinitis. *Clin. Allergy.* 3:411-425.
24. Weibel, E. R., and D. M. Gomez. 1962. A principle for counting tissue structures on random sections. *J. Appl. Physiol.* 17:343-348.
25. Williams, M. A. 1977. *Quantitative Methods in Biology.* North-Holland, New York. 5-84.
26. Williams, M. A. 1977. *Quantitative Methods in Biology.* North-Holland, New York. 85-169.